Motion Decoupling and Registration for 3D Magnetic Resonance Myocardial Perfusion Imaging

Nick Ablitt[1], Jianxin Gao[1], Peter Gatehouse[2], Guang-Zhong Yang[1,2]

[1]Royal Society/Wolfson Foundation MIC Laboratory, Imperial College, London, U.K.
[2]Royal Brompton Hospital, London, U.K.

{naa99,jxg,gzy@doc.ic.ac.uk}

Abstract. This paper presents a novel motion decoupling and registration method for 3D MR myocardial perfusion imaging. The technique uses tissue tagging for prospective through-plane motion correction of the left ventricle during 3D multi-slice image acquisition. The remaining in-plane distortion of the heart due to respiration was corrected by using a multi-resolution 2D free-form image registration method. Partial least square regression was adopted to recover the intrinsic relationship between respiration and cardiac deformation, both to speed up the registration process and to improve its internal consistency. Factor analysis is then applied to extract tracer characteristics of different regions of the myocardium. Both simulation data and *in vivo* images acquired from 8 normal subjects and 8 patients with coronary disease were used to validate the proposed techniques.

1. Introduction

Myocardial perfusion imaging is a valuable method in the evaluation of coronary artery disease. The technique is commonly performed in conjunction with coronary stress under coronary pharmacological vasodilatation when coronary blood flow is at its maximum. The technique provides several important haemodynamic parameters, including blood flow, volume, and mean transit time (the average time it takes for a tracer molecule to pass through the target tissue). The uptake of contrast agent within the myocardium is proportional to regional blood flow and the perfusion image series can be used to differentiate contrast agent uptake in regions of the myocardium supplied by normal or stenotic coronary arteries. The imaging method may be used to detect and distinguish between many different aspects of coronary heart disease. This includes ischaemia, infarction, reperfusion, myocardial viability, and detecting scar tissue in chronically infarcted myocardium. Traditionally, at the level of epicardial coronary arteries, angiographic anatomy is commonly used to identify hydraulically significant stenosis. At the level of coronary arteries, X-ray video-densitometry and electromagnetic and Doppler flow meters may be used to assess perfusion. Coronary venous thermodilution methods provide some insights into global or regional perfusion. At the arteriolar/capillary level, X-ray videodensitometer, contrast

P.M.A. Sloot et al. (Eds.): ICCS 2002, LNCS 2331, pp. 285–294, 2002.

echocardiography and microspheres may be employed. At the myocyte level, radionuclide and magnetic resonance imaging (MRI) methods can be used.

The recent development of MR myocardial perfusion imaging has extended the role of cardiovascular MRI in the evaluation of ischaemic heart disease beyond the situations where there have already been gross myocardial changes such as acute infarction or scarring. The ability to non-invasively evaluate cardiac perfusion abnormalities before pathologic effects occur, or as follow-up to therapy, is important to the management of patients with coronary artery disease. Early reperfusion of ischaemic myocardium has been shown to have a positive reversal effect on the ischaemic myocardium, which reduces mortality and morbidity. Differentiation of ischaemic but viable myocardium from infarcted regions requires detailed global quantitative assessment and modelling of myocardial perfusion characteristics. The prerequisite of such a study is the development of a spatially and temporally registered imaging strategy for a complete 3D coverage of the myocardium.

Hitherto, the assessment of myocardial perfusion using MRI has been based on first pass techniques using fast gradient echo (turboFLASH) [1-4] or echo-planar (EPI) sequences [5-7]. Quantitative results have been achieved in animal studies with intravascular agents (polylysine-Gd-DTPA)[8] as a macromolecular blood pool marker. At the same time, semi-quantitative results have also been established in human with conventional extracellular agents (Gd-DTPA) [9-11]. Either approach will have impact on detailed characterisation of the relationship between functional and perfusion abnormalities. Before comprehensive modelling can be achieved, however, it is necessary to address the imaging issues related to using MR for perfusion measurement. In 3D myocardial perfusion imaging, a complete volumetric data set has to be acquired for each cardiac cycle, and this can result in 150-300 such 3D data sets for studying the first pass of the contrast bolus. To ensure a comprehensive coverage of the myocardium and reasonably high resolution of the images, a typical data acquisition window of 100-200 *ms* per slice, and thus the overall acquisition time of more than 600 *ms* is required for each cardiac cycle to cover the entire volume of the left ventricle. When using multi-slice imaging, cardiac motion during this large acquisition window can cause the myocardium captured in different image planes to be mis-registered, *i.e.*, some parts of the myocardium may be imaged more than twice whereas other parts may be missed out completely. This type of mis-registration is difficult to correct by using post-processing techniques. With this study, we propose a novel motion decoupling technique based on motion tagging and real-time slice tracking. This resolves the movement of the myocardium along the long axis of the heart. A 2D free-form deformable model is then applied to correct for motion and deformation within image planes. By the use of motion decoupling, we turn the original four-dimensional problem (3D spatial + temporal) into multiple three-dimensional (2D spatial + temporal) subsets, and making this otherwise difficult task much more manageable.

2. Material and Methods

2.1 3D Motion Decoupling

Prior to perfusion imaging, a tagging sequence is used to highlight the short axis through plane motion of the heart. This consists of a vertical long axis (VLA) and horizontal long axis (HLA) tagged cine sequence within a single heartbeat, with the tag lines cutting through the short axis of the left ventricle (LV). The tags within these two cines are tracked throughout the cardiac cycle and a plane is fitted with least-mean-squares errors to the HLA and VLA short axis tag locations. The exact orientation of particular short axis planes within the myocardium is now known. Following from this, a standard multi-slice perfusion sequence is applied, which automatically adjusts the location and orientation of the imaging plane according to different trigger delays. The method assumes that the rate and extent of contraction of the LV is consistent between the motion tagging scan and subsequent perfusion imaging. The above procedures ensure that the through plane motion of the heart is captured during imaging. The decoupled in-plane motion can then be corrected for by using free-form 2D image registration techniques.

2.2 Free-Form Image Registration

The registration technique was adapted from our previous work on 2D electrophoresis image analysis [12]. It is a rapid multi-resolution free-form registration method based on a localized cross-correlation measure, as defined in Equation (1).

$$f(T)=\left|\frac{\sum_{\vec{x}\in\Omega}(I_1(\vec{x})-E\{I_1(\vec{x})\})(I_2(T(\vec{x}))-E\{I_2(T(\vec{x}))\})}{\sqrt{\sum_{\vec{x}\in\Omega}(I_1(\vec{x})-E\{I_1(\vec{x})\})^2}\sqrt{\sum_{\vec{x}\in\Omega}(I_2(T(\vec{x}))-E\{I_2(T(\vec{x}))\})^2}}\right| \quad (1)$$

where T is the applied deformation and Ω the overlapping pixels in the intersection region of the reference (I_1) and the transformed image (I_2). A linear tensor product B-spline as defined in Equation (2) was subsequently used as the transformation matrix as it enables adaptive automatic subdivision of the control grids when increasing the resolution, *i.e.*

$$T(\vec{p})=\sum_{i,j}\beta_{ij}(u,v)\vec{c}_{ij} \quad (2)$$

where $\beta_{ij}(u,v)$ is the coefficient applied to point $\vec{p}(u,v)$, and $\vec{c}_{ij}$ is the coordinate of control points surrounding $\vec{p}(u,v)$. The use of Equation (1) allows a close-form derivation of the derivatives of the similarity function such that quasi-Newton optimization techniques can be effectively used. The BFGS algorithm was used in this study to determine the optimum deformation vector of each grid control point with the following updating equations

$$x_{k+1} = x_k - H_k^{-1}\nabla f(x_k),$$
$$s_k = x_{k+1} - x_k, \quad y_k = \nabla f(x_{k+1}) - \nabla f(x_k), \tag{3}$$
$$H_{k+1} = H_k + \frac{y_k y_k^T}{y_k^T s_k} - \frac{H_k s_k s_k^T H_k}{s_k^T H_k s_k}$$

where H_k is the estimated Hessian matrix, and $\nabla f(x_k)$ is the vector of partial derivative of the function with respect to each parameter of T, dictated by the grid control points. In this study, the reference image was chosen to be at the end of the image series as all cardiac structures were clearly identifiable. Each image of the perfusion sequence was then registered to the reference image with a final grid resolution of 10×10.

2.3 Self-adaptive Learning and Prediction with Partial Least Squares Regression

After 3D motion decoupling with prospective slice tracking, the residual in-plane myocardial deformation is restricted to those caused by respiration. It is possible to exploit subject-specific near-linear relationships between respiration and cardiac deformation to increase the internal consistency of the registration process or to use the pattern of respiration as a prediction of myocardial deformation. To this end, the user is required to identify regions on one perfusion image, either through the chest or the diaphragm, where respiratory induced cyclic motion could be retrospectively recovered. The signals from these regions formed navigator traces and a partial least squares regression (PLSR) algorithm was used to recover the pattern of respiratory motion and the associated myocardial deformation extracted by the above free-form image registration process.

Let **X** and **Y** denote the respiratory motion and free-form deformation, respectively. The intrinsic relationship can be expressed as

$$\mathbf{Y = XC + E} \tag{4}$$

where **C** is the coefficient matrix, and **E** represents noise and higher order terms. In PLSR, both the input **X** and output **Y** are used for extracting the factors in forming the coefficient matrix **C**. To do so, **X** and **Y** are decomposed as

$$\mathbf{X = TP + E_1}$$
$$\mathbf{Y = TQ + E_2} \tag{5}$$

In Equation (5), **T** is the factor score matrix, **P** the factor loading matrix, **Q** the coefficient loading matrix, $\mathbf{E_1}$ and $\mathbf{E_2}$ represent, respectively, parts of **X** and **Y** that are unaccounted for. The latent vectors are the eigenvectors of the covariance matrix **(X'Y)'(X'Y),** through which a weighting matrix **W** can be computed iteratively such that **T=XW**. Once **P**, **Q** and **W** are found, the regression matrix in equation (4) can be determined as **C=WQ** [13]. In the current study, we used 30% of the image frames located at the end of the perfusion sequence for learning and extracting the regression matrix **C** using the first 4 principal components of the covariance matrix. Deformation fields for the remaining images were derived from the PLSR prediction.

2.4 Extraction of Regional Perfusion Abnormality with Factor Analysis

For the quantification of regional perfusion abnormality, both model-based and modeless approaches can be used. For the model-based approaches, tracer kinetics is commonly assumed to follow a Fermi function [14]. By using the intensity variation measured from the LV blood pool as the input signal, deconvolution is required to recover the impulse response of different regions of the myocardium. In practice, the signal from the LV blood pool may be significantly attenuated at peak amplitude due to the relatively high concentration of the Gd-DTPA used. In this case, the model based approach can introduce significant errors. Furthermore, the use of a single model for representing both normal and infracted regions requires further justification. In this study, factor analysis for dynamic image series was used to determine regional perfusion abnormalities.

Factor analysis is a valuable tool for extracting underlying characteristics of a region of interest (ROI) with different tissue types from dynamic image series without prior assumptions about tissue models. An image sequence S can be represented as the sum of K underlying images (spatial distribution) a_k, each weighted by their factors (temporal distribution) f_k, as follows [15-16],

$$S(p,t) = \sum_{k=1}^{K} a_k(p) \cdot f_k(t) + e(p,t) \tag{6}$$

where $e(p,t)$ is the residual error and K is the number of factors kept, usually is equal to the number of different tissue kinetics within the ROI. By neglecting the error term, the above expression can be turned into a matrix form

$$\mathbf{S} = \mathbf{FA} = \mathbf{U}\tilde{\mathbf{A}}\mathbf{V} \tag{7}$$

where $\mathbf{S}$ is a M×N matrix, $\mathbf{U}$ the M×K orthonormal column matrix composed of the first K principal kinetic curves, $\mathbf{V}$ the K×N orthonormal row matrix composed of K principal component images, $\tilde{\mathbf{A}}$ the K×K diagonal matrix of the K roots of eigenvalue, M and N are the number of image frames and total number of pixels within the ROI, respectively. Since there is no unique solution to the above equation, additional constrains are necessary. Among them, the positive constraint is the most commonly adopted one. It is based on the fact that there are no negative values in the actual images and the corresponding time curves, *i.e.*, factors. This can be implemented by iterative oblique rotations of the factors and the corresponding factor images.

2.5 Validation and *in vivo* Data Acquisition

To assess the accuracy of the proposed techniques, both numerical simulation and *in vivo* data sets were used. For the synthetic dataset, the signal characteristics were generated based on an idealised myocardial first-pass perfusion model and a typical respiration pattern derived from normal subjects. The model includes two artificial defects in different parts of the myocardium, and this dataset is used to evaluate the proposed 2D free form registration, self-adaptive learning and prediction with PLSR, and perfusion characterisation based on factor analysis. *In vivo* results were acquired

from both normal volunteers and patients with known coronary artery disease. These images were obtained using a 1.5T Siemens Sonata scanner (200 *T/m/s*; 40 *mT/m*) with a four-element phased-array receiver coil. For 3D tracking, the HLA and VLA tagged cine images were obtained in the same 16-cycle end-expiratory breath-hold, using segmented FLASH imaging. In each cardiac cycle, a multiplanar ("comb") saturation pulse was applied after the R-wave to tag the myocardium parallel to the short axis of the heart. The first-pass perfusion data was acquired from 8 patients with a FLASH sequence (Tr=3.7 *ms*) that consists of three saturation-recovery short-axis slices per cardiac cycle, for 50 cycles during the first-pass of Gd-DTPA (cubital vein, 0.1 *mmol/kg*, 3 *ml/s*) with a field of view of 400 *mm* (128 pixels) by 300 *mm* (64 pixels).

In addition to these, a special test pulse sequence was developed to examine the accuracy of the proposed prospective tracking method for 3D motion decoupling. The sequence used the same tagging pre-pulse as before, but the imaging part of the sequence was altered such that it imaged the same basal plane three times at 156 *ms* intervals. When slice tracking was enabled, the acquired images would always be in alignment with the tagging plane, and therefore the signal from the myocardium would be nullified. Otherwise, the acquired images would cover different parts of the myocardium, and therefore had an uneven intensity distribution. For the purpose of visualization, these images were subtracted from their counter parts without the use of the tagging pre-pulse. In this case, the intensity distribution of the myocardium would be uniformly bright if slice tracking had been accurate. Three normal subjects were studied for this purpose. A further study of five normal volunteers was carried out for 3D motion decoupling with a normal perfusion sequence but without the administration of Gd-DTPA bolus.

3. Results

Figure 1 illustrates one example of the slice tracking process for motion decoupling on one of the normal subjects studied. The first and second rows show the VLA and HLA images of the heart at three different phases of the cardiac cycle. The darker and brighter pilot grids illustrate the imaging planes in which the myocardium would be covered with and without motion tracking, respectively. The resultant short axis images acquired by the special test pulse sequence are shown at the two bottom rows. Without tracking, the acquired images covered different parts of the myocardium as indicated by both intra and inter-phase signal variations of the myocardium. By the use of effective slice tracking, the same part of the myocardium was always covered by the same image plane, resulting in a consistent intensity distribution within the myocardium. For the three subjects verified, the percentage changes in signal intensity varied from –59% to 74% (absolute mean±std = 45±9.8%) without tracking, and –9% to 22% (absolute mean±std = 9±3.9%) with tracking. For 3D motion decoupling based on the normal perfusion sequence, areas of the myocardium of the LV were measured for the five normal subjects studied. The three short axis slices were taken within the same cardiac cycle, with the most apical slice acquired first and

the most basal slice last. The bar chart shown in Figure 2 indicates the absolute differences of measured regional errors in mm^2 without motion tracking.

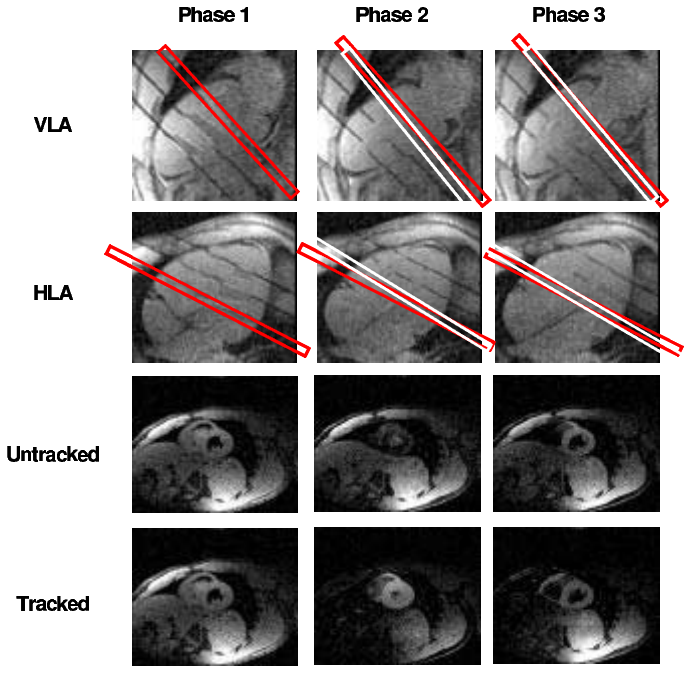

Fig 1. A schematic illustration of the basic procedures used for prospective tracking of through plane cardiac motion. Cine myocardial tagging is performed on both the VLA and HLA of the LV from which the positions of the tracking planes are derived. The two bottom rows demonstrate the effectiveness of slice tracking by using a special test pulse sequence. Signals form the myocardium should remain uniform if the imaging planes are accurately tracked over time.

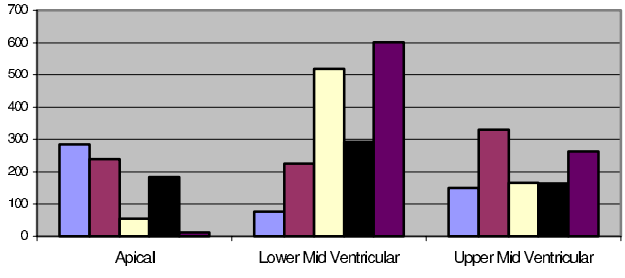

Fig 2. The amount of motion involved for the apical, lower and upper mid-ventricular slices measured from five normal subjects by using the short-axis area change as an indicator.

Figure 3 demonstrates the effectiveness of image registration by using the predicted myocardial deformation based on adaptive self-learning with PLSR. It shows an example of the effect of the registration on the resulting time series curves with the deformation grid superimposed onto the original perfusion images. For the 8 patients studied, four perfusion signal time curves were measured at the Anterior, Posterior, Septal, and Lateral Segments for each perfusion sequence. Spline curve fitting was applied to each of these curves and the mean dispersion was used as an objective measure of the accuracy of the registration method. With the simulation data set, the mean dispersion is reduced to about 85% of its original value by using the free-form registration procedure. With PLSR training, this error is further reduced (77%) while the actual computation time is halved. For the 8 patient data sets analyzed, the mean dispersion was reduced to 81% and 68%, respectively, by using the free-form registration method and the PLSR approach.

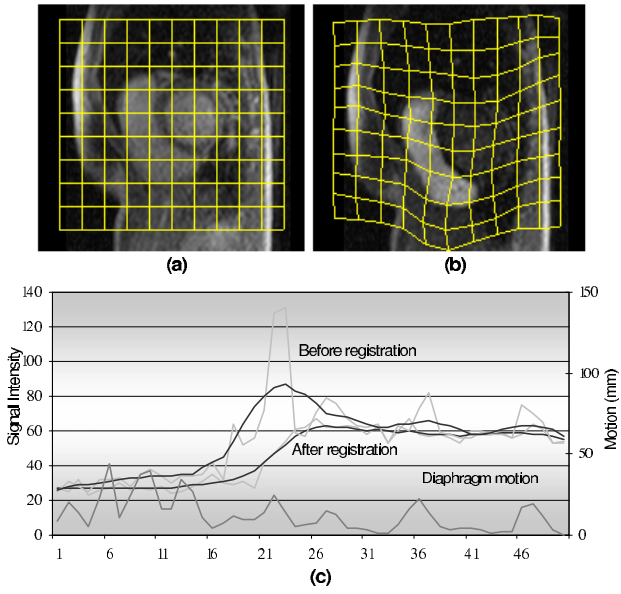

Fig 3. The layout of the control grid used for correcting free-form in-plan deformation due to respiration, (a) reference, and (b) target image with superimposed deformation field. The effect of motion correction with PLSR is shown in (c) where signal dispersion in relation to the spline fitted curve is used as a measure of the accuracy of the registration process. The example perfusion curves were measured at the Septal Segment for one of the patients studied.

Figure 4 shows 8 time frames of the synthetic perfusion images with a lateral sub-endocardial defect and another posterior transmural defect. The first three factor images of the perfusion sequence clearly indicate different tracer kinetic behaviours of the myocardium and the exact locations of the defects.

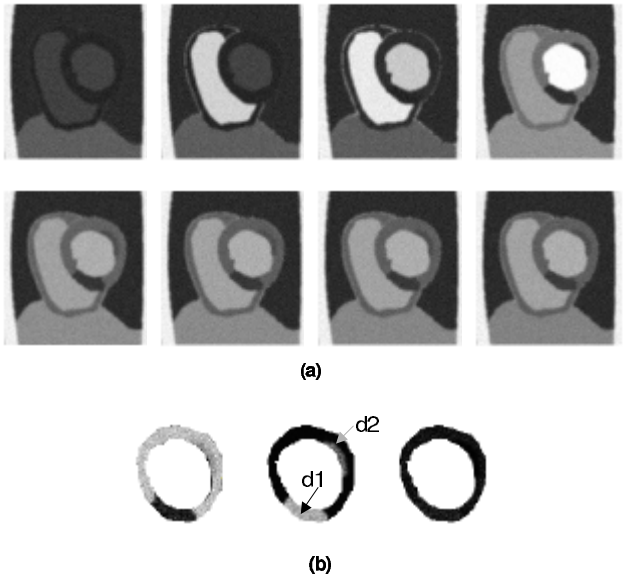

Fig 4. (a) Eight image frames from a synthetic perfusion sequence showing both sub-endocardial and transmural perfusion defects. (b) The derived factor images show different tracer characteristics of the myocardium and the locations of the defects (d1 and d2, pointed by the arrows).

4. Discussion and Conclusions

Magnetic resonance myocardial perfusion imaging is a promising method in the evaluation of coronary artery disease. Existing techniques for first-pass myocardial perfusion imaging analysis normally involve either single or multiple un-registered imaging planes based on manual delineation of ROIs at different regions of the myocardium. In-plane deformation can be restored to some extent by the labor-intensive manual correction process, albeit being error prone. The through plane cardiac motion due to extended imaging time involved in 3D perfusion imaging, however, is not recoverable by post-processing. The use of 3D motion decoupling effectively resolves this problem. It ensures the material captured by each imaging plane always covers the same part of the myocardium. The use of 2D free-form image registration removes any in-plane distortion and makes subsequent perfusion quantification fully automatic. Another major innovation of the current study is the use of PLSR for self-adaptive learning of subject-specific cardiac motion induced by respiratory motion. It has been shown that it not only substantially reduces the number of imaging frames to be registered but also makes the motion correction results much more consistent. Quantification is of significant importance in myocardial perfusion imaging as it allows the evaluation of further aspects of perfusion such as myocardial viability. Currently, there is very little evidence of the reproducibility of results. This paper presents a practical way of obtaining 3D

registered perfusion sequence that are essential for further quantitative modelling of regional perfusion abnormalities.

References

1. Wilke N, Simm C, Zhang J, Ellermann J, Ya X, Merkle H, Path G, Ludemann H, Bache RJ, Ugurbil K. Contrast-enhanced first pass myocardial perfusion imaging: correlation between myocardial blood flow in dogs at rest and during hyperemia. *Magn Reson Med.* 1993;29(4): 485-97.
2. Wilke N, Jerosch-Herold M, Stillman AE, Kroll K, Tsekos N, Merkle H, Parrish T, Hu X, Wang Y, Bassingthwaighte J, et al. Concepts of myocardial perfusion imaging in magnetic resonance imaging. *Magn Reson Q.* 1994;10(4): 249-86.
3. Cullen JH, Horsfield MA, Reek CR, Cherryman GR, Barnett DB, Samani NJ. A myocardial perfusion reserve index in humans using first-pass contrast-enhanced magnetic resonance imaging. J *Am Coll Cardiol.* 1999;33: 1386-94.
4. Keijer JT, van Rossum AC, van Eenige MJ, Karreman AJ, Hofman MB, Valk J, Visser CA. Semiquantitation of regional myocardial blood flow in normal human subjects by first-pass magnetic resonance imaging. *Am Heart J.* 1995; 130:893-901.
5. Schwitter J, Debatin JF, von Schulthess GK, McKinnon GC. Normal myocardial perfusion assessed with multishot echo-planar imaging. *Magn Reson Med.* 1997;37(1): 140-7.
6. Beache GM, Kulke SF, Kantor HL, Niemi P, Campbell TA, Chesler DA, Gewirtz H, Rosen BR, Brady TJ, Weisskoff RM. Imaging perfusion deficits in ischemic heart disease with susceptibility-enhanced T2-weighted MRI: preliminary human studies. *Magn Reson Imaging.* 1998;16(1): 19-27.
7. Ding S, Wolff SD, Epstein FH. Improved coverage in dynamic contrast-enhanced cardiac MRI using interleaved gradient-echo EPI. *Magn Reson Med.* 1998;39(4): 514-9.
8. Wilke N, Kroll K, Merkle H, Wang Y, Ishibashi Y, Xu Y, Zhang J, Jerosch-Herold M, Muhler A, Stillman AE, et al. Regional myocardial blood volume and flow: first-pass MR imaging with polylysine-Gd-DTPA. *J Magn Reson Imaging.* 1995;5(2): 227-37.
9. Larsson HBW, Stubgaard M, Søndergaard L, Henriksen O. In vivo quantification of the unidirectional influx constant for Gd-DTPA diffusion across the myocardial capillaries with MR imaging. *J Magn Reson Imaging.* 1994; 4: 433-40.
10. Dendale P, Franken PR, Block P, Pratikakis Y, De Roos A. Contrast enhanced and functional magnetic resonance imaging for the detection of viable myocardium after infarction. *Am Heart J.* 1998; 135: 875-80.
11. Larsson HBW, Fritz-Hansen T, Rostrup Egill, Søndergaard L, Ring P, Henriksen O. Myocardial perfusion modeling using MRI. *Magn Reson Med.* 1996; 35: 716-26.
12. Veeser S, Dunn MJ, Yang GZ. Multiresolution image registration for two-dimensional gel electrophoresis. *Proteomics.* 2001; 1: 856-870.
13. Wold, H. Soft modelling with latent variables: the nonlinear iterative partial least squares approach. Perspectives in probability and Statistics: Papers in honour of M.S. Barlett, (J. Gani, ed). London: Academic Press. 1975: 114-142.
14. Jerosch-Herold, M, Wilke N, Stillman AE. Magnetic resonance quantification of the myocardial perfusion reserve with a Fermi function model for constrained deconvolution, *Medical Physics,* 1998; 25: 73-84.
15. Buvat I, Benali H, Paola RD. Statistical distribution of factors and factor images in factor analysis of medical image sequences. *Phys Med Biol.* 1998; 43: 1695–1711.
16. Martel AL, Moody AR, Allder SJ, Delay GS, Morgan PS. Extracting parametric images from dynamic contrast-enhanced MRI studies of the brain using factor analysis. *Med Img Analysis,* 2001; 5: 29-39.